Orientation and Dynamics of Myosin Heads in Aluminum Fluoride Induced Pre-Power Stroke States: An EPR Study[†]

Dražen Raucher and Piotr G. Fajer[*]

Institute of Molecular Biophysics and Department of Biological Science, Florida State University, Tallahassee, Florida 32306

ABSTRACT: We have determined the orientation and dynamics of the putative pre-power stroke crossbridges in skinned muscle fibers labeled with maleimide spin-label at Cys-707 of myosin. Orientation was measured using electron paramagnetic resonance (EPR) and mobility by saturation transfer EPR. The crossbridges are trapped in the pre-power stroke conformation in the presence of aluminum fluoride, Ca, and ATP. In agreement with data published for unlabeled fibers (Chase et al., 1994), spin-labeled muscle fibers display 42.5% of rigor stiffness, without the generation of force. The trapped crossbridges are as disordered as the relaxed heads, but their microsecond dynamics are significantly restricted. Modeling of the immobile fraction (35%), in terms of attached heads as estimated from stiffness, suggests that the bound heads rotate with a correlation time $\tau_r = 150–400$ μs, as compared to $\tau_r = 3$ μs for the heads in relaxed fibers. These "strongly" attached myosin heads, at orientations other than in rigor, are a candidate for the state from which head rotation generates force, as postulated by H. E. Huxley (1969). Ordering of the heads may well be the structural event driving the generation of force.

Force generation in muscle is thought to arise by the rotation of an actin-attached myosin head (or of a portion of a myosin head) (Huxley, 1969; Rayment et al., 1993), thereby creating strain which is relieved by the sliding of the thin and thick filaments. The actual molecular mechanism of force generation though is still unclear. The strongest evidence comes from a comparison of myosin head orientations in the various stages of the biochemical cycle, which drives the structural changes. Before attachment to actin, the heads are disordered without an identifiable preferred orientation, while in the rigor state (which corresponds to the post-power stroke conformation) the heads are attached at 40–45° [see Pollard et al. (1993) and references cited therein]. The intermediate attached states are less well-defined; during the initial weak binding, the heads are as disordered as the detached states (Fajer et al., 1991; Pate et al., 1992; Frado & Craig, 1992), but these heads are in a dynamic equilibrium between attached and detached states, and are thus unlikely to generate force [reviewed by Schoenberg (1993)]. Previous attempts to trap the contractile cycle in the "strongly bound" (slowly dissociating) intermediates, corresponding to the pre-power stroke state, have proved to be inconclusive. In the presence of the nonhydrolyzable adenosine 5′-triphosphate (ATP)[1] analog AMPPNP, some muscles indeed display an orientation different from that of rigor (Tregear et al., 1990), while in other muscle types, AMPPNP or PP$_i$ induces a single-headed crossbridge, with a mixture of rigor- and relaxed-like heads

(Fajer et al., 1988; Pate & Cooke, 1988). Myosin heads in isometrically contracting fibers also show little or no preferred orientation (Fajer et al., 1990b; Hirose & Goldman, 1993), as expected from heads undergoing large-amplitude microsecond motions (Barnett & Thomas, 1989; Stein et al., 1990; Berger & Thomas, 1993). However, in the steady-state contraction, the pre-power stroke states might be short-lived and not significantly populated. It is therefore of help to seek conditions in which the steady-state population of heads is biased toward "strongly bound", non-force-producing states.

The metallofluoride complexes are thought to be high-affinity analogs of inorganic phosphate. Aluminum fluoride and beryllium fluoride, like orthovanadate, can form a stable complex with myosin subfragment 1 (S1) in the presence of MgADP (Werber et al., 1993). Spectroscopic and biochemical evidence has established similarities between actomyosin-aluminate and beryllate complexes, and the AM**·ADP·P$_i$ complex (Maruta et al., 1993; Phan et al., 1993). In muscle fibers, aluminum fluoride causes a strong inhibition of force generation, without a parallel inhibition of stiffness (Chase et al., 1994), indicating that aluminum fluoride traps cycling heads in the pre-power stroke conformation. In this study, we have determined the orientation and dynamics of these trapped myosin heads using saturation transfer and conventional EPR techniques. The heads in the pre-power stroke state are as disordered as detached heads, but their mobility is highly restricted. A similar disordering of the putative pre-power stroke heads was observed in the presence of butadione monoxime, as described by Zhao and Cooke (1994a).

MATERIALS AND METHODS

Sample Preparation. New Zealand white rabbits (~4 kg) were sacrificed by CO_2 asphyxiation or by anesthetization with 75 mg of ketamine hydrochloride/kg weight, and small strips of psoas muscle (~2 mm diameter) were removed. The fiber bundles were incubated at 4 °C on a shaker in a glycerinating solution (60 mM KOAc, 2 mM MgCl$_2$, 10 mM EGTA, 25 mM MOPS, 1 mM NaN$_3$, and 25% glycerol, pH 7) for 24 h, and then transferred to fiber storage solution (60

[*] To whom correspondence should be addressed.

[®] Abstract published in *Advance ACS Abstracts,* September 1, 1994.

[1] Abbreviations: AMPPNP, adenosine 5′-(β,γ-imidotriphosphate); ATP, adenosine 5′-triphosphate; ATP-γ-S, adenosine 5′-*O*-(3-thiotriphosphate); CPK, creatine phosphokinase; EDTA, ethylenediaminetetraacetic acid; EGTA, ethylene glycol bis(β-aminoethyl ether)-*N,N,N′,N′*-tetraacetic acid; IASL, (2,2,6,6-tetramethyl-4-piperidinyl)iodoacetamide; MOPS, 3-(*N*-morpholino)propanesulfonic acid; MSL, *N*-(1-oxy-2,2,5,5-tetramethyl-4-piperidinyl)maleimide; PCr, phosphocreatine; EPR, electron paramagnetic resonance; ST-EPR, saturation transfer electron paramagnetic resonance; S1, myosin subfragment 1.

mM KOAc, 2 mM $MgCl_2$, 1 mM EGTA, 25 mM MOPS, and 1 mM NaN_3 plus 50% glycerol, pH 7) for 48 h prior to storage at -20 °C. Subfragment 1 (S1) was prepared from myosin by digestion with α-chymotrypsin in 120 mM KCl, 10 mM MOPS, and 1 mM EDTA, pH 7, as described by Weeds and Taylor (1975) and stored at -70 °C prior to use.

Standard solutions for fiber experiments contained 1 mM EGTA, 15 mM PCr, 5 mM MgATP, 3 mM $MgCl_2$, and 250 units/mL CPK at 20 °C; the ionic strength was adjusted to 0.17 M with potassium propionate. Activating solution contained 1.5 mM $CaCl_2$. All solutions were buffered with 40 mM MOPS at pH 7.0. Aluminum fluoride was formed by the addition of 10 mM NaF and 3 mM $AlCl_3$.

Electron Paramagnetic Resonance. EPR experiments were performed on a Bruker ECS-106 spectrometer (Bruker Inc., Billerica, MA), using a TM_{110} cavity, modified to accept a fiber-containing capillary parallel to the static magnetic field. EPR spectra were transferred to an IBM-compatible personal computer and analyzed with software developed by the authors. Conventional EPR spectra were acquired at 100 kHz modulation frequency, 1.0 G modulation amplitude, 9.81 GHz microwave field frequency, and a microwave field intensity, $H_1 = 0.144$ G. Saturation transfer EPR (ST-EPR) spectra (second harmonic absorption, out-of-phase) were acquired with a microwave field intensity $H_1 = 0.18$ G, a modulation amplitude of 5 G, and a modulation frequency of 50 kHz. The instrument was calibrated with peroxylamine disulfonate (1 mg/mL) in 50 mM K_2CO_3, as described previously (Fajer & Marsh, 1982). Calibration curves for ST-EPR spectra were generated from deoxyhemoglobin tumbling in 88% (w/w) mixtures of glycerol and water (Thomas *et al.*, 1976; Fajer & Marsh, 1982; Squire & Thomas, 1986).

Mechanical Measurements. The force generated by a single fiber was measured using a Cambridge force transducer (Model 300A; Cambridge Technology Inc., Watertown, MA), and normalized to the fiber area as estimated by measuring the fiber diameter (60–80 μm) at five locations along the fiber. The isometric tension at 20 °C was found to be 1.75 $\pm$ 0.1 kg/cm^2 for unlabeled fibers and 1.6 $\pm$ 0.1 kg/cm^2 for spin-labeled samples (B. Adhikari, private communication). Fiber stiffness was measured using a force transducer and a length driver (Cambridge Technology Inc.), interfaced to a personal computer, and controlled by a program (DAC) developed at the University of Washington (Seattle). For each measurement, the fiber length was changed in steps of 0.5, 0.7, 0.9, 1.1, and 1.3% of the fiber length (2–3 mm). The steps were completed within 0.3 ms, and the fiber force was recorded 12 ms after the step-length perturbation. The data were analyzed with software developed by the authors.

RESULTS

Stiffness. The attachment of the myosin heads to actin was determined by muscle stiffness. Figure 1 shows fiber resistance to stretches of increasing length. In the presence of 5 mM MgATP, the fibers are relaxed and offer little resistance to the length perturbations. In the absence of any nucleotides (rigor), the fibers are stiff and strongly resist any length changes. Since the viscoelastic properties of the filaments are not likely to be affected by the presence of MgATP, fiber stiffness is commonly used as a measure of myosin attachment (Ford *et al.*, 1981). Although there is a strong suggestion that the stiffness of a single-headed cross-bridge can be the same as that of a crossbridge in which both myosin heads are attached (Fajer *et al.*, 1988; Pate & Cooke, 1988), there is little doubt that stiffness reflects crossbridge
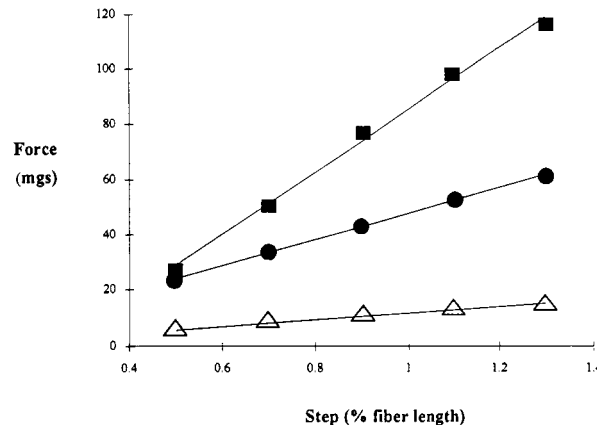

FIGURE 1: Fiber stiffness as measured by the slope of the force response to the imposed length stretch: ($\triangle$) relaxation, 5 mM ATP; ($\blacksquare$) rigor; ($\bullet$) aluminum fluoride and Ca^{2+}. Tension response was measured 12 ms after each length change.

attachment, be it a single- or a double-headed crossbridge. Assuming 100% myosin head attachment in rigor (Offer & Elliot, 1978; Thomas & Cooke, 1980), and crossbridge elasticity independent of the chemical state of the head, the extent of attachment is calculated from the fractional stiffness with respect to the stiffness in rigor. Since the force is determined 12 ms after the completion of the length change, the crossbridges contributing to the force response are long-lived, i.e., "strongly attached" crossbridges, as distinguished from transient "weak" crossbridges, such as those seen at low ionic strength, low-temperature relaxation (Schoenberg, 1993).

From the slope of the force response in Figure 1, we can thus estimate that 4.8% of the myosin heads are attached in relaxation, and also in the presence of AlF_3 without added Ca^{2+} (data not shown). This increases to 42.5% in the presence of AlF_3 plus Ca^{2+} (see Table 1). This crossbridge formation is not, however, accompanied by the generation of force, as in contraction. A fraction of the myosin heads seem to be trapped in the "strongly" attached state prior to the tension-generating step, as originally proposed by Chase and co-workers (Chase *et al.*, 1994).

Orientation. In order to determine the orientational distribution of the myosin heads, we have performed EPR measurements on muscle fiber bundles labeled with MSL. The conventional EPR spectra shown in Figure 2 were obtained for fibers parallel and perpendicular to the direction of the magnetic field. The narrow line width of the MSL spectrum (3.6 G) indicates a high level of ordering, translating into a $\pm 7°$ Gaussian disorder of the myosin heads (Fajer *et al.*, 1990a). As we have shown recently (Fajer, 1994), the orientation of the nitroxide ring within the myosin head (as determined from the hyperfine splitting) assures a fairly high sensitivity to any axial reorientation of the myosin head about its mean rigor position. Upon relaxation with 5 mM MgATP, the heads become dynamically disordered (Barnett & Thomas, 1984), and the EPR lineshape becomes nearly isotropic (Figure 2b). The myosin heads are, however, not completely disordered, as demonstrated by the difference between the spectra taken at two orientations with respect to the magnetic field (see Figure 2b,f). The addition of AlF_3 to relaxed fibers resulted in no spectral change at either orientation of the sample (data not shown), consistent with all of the crossbridges being in the detached state (Figure 1). A similar disordering of the heads was observed in X-ray diffraction patterns of fibers incubated with AlF_3 in the absence of Ca^{2+} (Schrumpf & Wray, 1992).

Table 1: Properties of Myosin Heads in AlF_3[a]

state	stiffness (% fraction of rigor)	force (kg/cm²)	EPR (% fraction of rigor)	ST-EPR (% fraction of rigor)
relaxation	4.9 ± 0.7	0	0	0
rigor	100		100	100
contraction	71 ± 8	1.9 ± 0.1	$4-12$[b]	13^d-22[c]
$ATP + AlF_3$	4.8 ± 0.8	<0.1	<2	<2
$ATP + AlF_3 + Ca^{2+}$	42.5 ± 3.1	<0.1	<2	35.0 ± 5.1

[a] Errors are SEM from 6–9 independent measurements. [b] From Fajer *et al.* (1990b). [c] From Barnett and Thomas (1989). [d] Adhikari and Fajer (1995), private communication.

FIGURE 2: Conventional EPR spectra of muscle fibers labeled with MSL and placed parallel (*left*) and perpendicular (*right*) to the magnetic field. Rigor fibers (*a, e*); relaxed (*b, f*); in AlF_3 and Ca (*c, g*). Difference between spectra in relaxation and in AlF_3+Ca (*d, h*).

The addition of Ca^{2+} to AlF_3–ATP fibers also resulted in no spectral change. The EPR spectra in the presence of Ca^{2+} and AlF_3 were identical to the spectra of relaxed fibers (see Figure 2c,g). The difference spectra confirm a nearly identical orientational distribution in these two cases. This is very surprising, since 42% of all available crossbridges are bound under these conditions as measured by stiffness (Table 1), suggesting that the bound heads are attached in many different orientations.

Mobility. Dynamics is an important aspect of myosin head behavior. We have used the saturation transfer EPR technique, which offers sensitivity to rotational motions extending from 0.1 μs to 1 ms. This motional region is believed to span the rates of myosin head motions, when attached to, or detached from, the thin filaments (Thomas *et al.*, 1980). The rigor spectra in Figure 3a are characteristic of the rigid limit of the dynamic range indicating no microsecond mobility, as described originally by Thomas *et al.* (1980). The large values of the diagnostic intensities at positions L″, C′, and H″, and the high integrated intensity of the ST-EPR spectrum, are similar to those of a globular protein undergoing Brownian diffusion with a correlation time of 2–3 ms.

Relaxation in the presence of ATP is accompanied by the onset of microsecond motion, which decreases the ST-EPR integrated intensity, and results in a decrease of the diagnostic intensities; e.g., the C′ value becomes negative (Figure 3b). The correlation time is 3 μs, as estimated from hemoglobin reference spectra. This microsecond motion is characteristic for detached heads, and is visible in stretched fibers in the absence of nucleotides (Barnett & Thomas, 1984). The
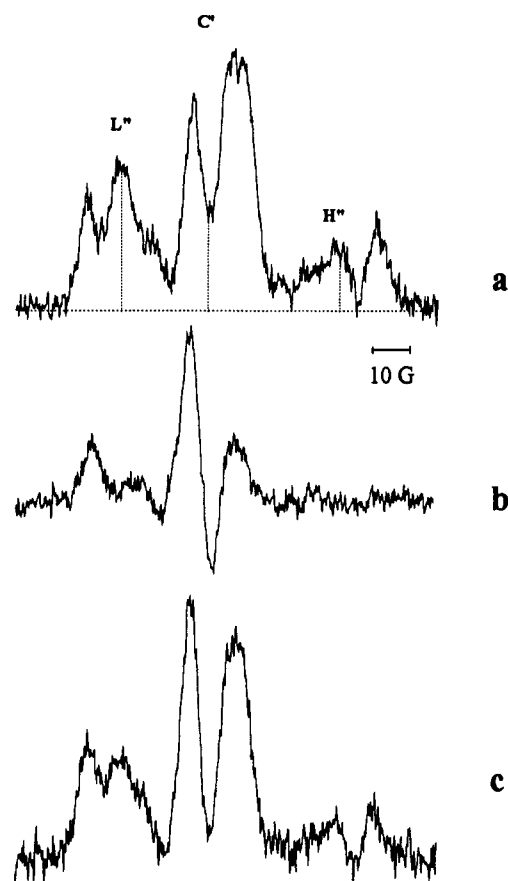

FIGURE 3: Saturation transfer spectra of MSL-labeled fibers: (*a*) rigor fibers; (*b*) relaxation; (*c*) AlF_3 and Ca^{2+}.

addition of AlF_3 in the presence of ATP resulted in no spectral changes (data not shown), consistent with the absence of any effects on fiber stiffness or head orientation. This is contrasted with the effects of AlF_3 plus Ca^{2+} (Figure 3c). The spectrum is now intermediate between that of rigor and relaxation, and it can be expressed as a linear combination of the two. The 35% fraction of the rigorlike immobile heads approaches that of the 42.5% fraction of rigor stiffness (Table 1), suggesting that the heads contributing to stiffness are significantly immobilized.

Strength of Binding. An independent verification of the disordering of attached heads is obtained from the retention of the extrinsic labeled S1 heads decorating an unlabeled fiber. This experiment allows the simultaneous measurement of orientation and attachment of infused myosin heads. In the absence of any nucleotide, the EPR spectrum is a composite of the spectrum of the heads making rigor bonds with the thin filaments and the spectrum of the unbound heads in the void volume of the sample capillary. The two species are spectrally resolved, the former contributing to the intensity at P_2, while
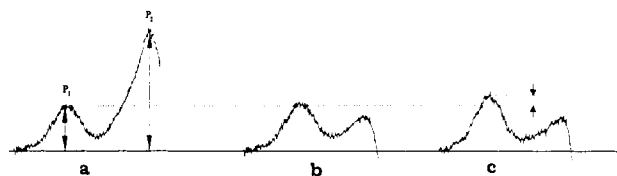
FIGURE 4: EPR spectra of unlabeled muscle fibers irrigated with MSL-labeled S1 fragments. The P_i intensity denotes the concentration of disordered myosin heads (free and bound); P_2 is a measure of the amount of heads bound in the rigor conformation. (a) Rigor; (b) heads relaxed with 5 mM MgATP; (c) AlF$_3$/Ca in the presence of 5 mM MgATP. The sample was placed parallel to the magnetic field.

the unbound S1 is tumbling isotropically in solution and contributes to P_1 (Figure 4). The signal intensity at these positions is reflecting the concentration of the ordered and disordered heads. Due to the narrower line width of the ordered fraction, the line height at P_2 is 2.65 times bigger than at P_1 for equimolar spin concentrations. The free S1 fraction is at equilibrium with a large reservoir of 80 μM S1, which is being pumped continually through the sample capillary. On the addition of 5 mM ATP, the intensity at P_2 decreases to the level expected for 80 μM free S1 without an increase of the P_1 intensity, implying that the detached heads equilibrate quickly with the reservoir without being trapped in the fiber lattice (Figure 4b). In the presence of AlF$_3$ and Ca^{2+}, the P_2 intensity diminishes as before, but the P_1 intensity increases (Figure 4c), suggesting that most of the bound heads detached and equilibrated with the reservoir but a substantial fraction (18%) became disordered and remained attached. This fraction is lower than that estimated from the fiber stiffness, since the intrinsic heads experience a higher effective actin concentration (Fajer et al., 1988).

These disordered, attached heads are in a very slow on–off equilibrium, and can be washed out of the fiber with AlF$_3$/Ca^{2+} (no S1) buffer over a period of 1 h. The rate of observed detachment is not limited by the diffusion of the S1 out of the fiber (Kraft et al., 1992), since a complete washout was achieved in less than 5 min in the presence of 5 mM MgATP.

DISCUSSION

We have shown that in the presence of AlF$_3$ and ATP, labeled myosin heads are dynamically disordered, as expected from detached crossbridges. The addition of Ca^{2+} resulted in "strong" attachment of the myosin heads, as measured by either mechanical stiffness or diffusion of the labeled S1 fragments from decorated muscle fibers. These bound heads displayed identical, nearly isotropic orientational distribution as the relaxed heads; however, their mobility was severely restricted. Thus, insofar that AlF$_3$/Ca^{2+} is an analog of the pre-power stroke, the heads prior to force generation are more statically disordered, in contrast to the dynamic disorder of weakly immobilized heads, and in contrast to the high order and immobilization of the post-power stroke myosin heads (in ADP or in rigor). We can speculate that the heads following attachment undergo a sequence of steps with progressively stronger binding to actin, accompanied by restriction of motional freedom. "Strongly" attached heads have restricted microsecond mobility, but they still display a wide range of orientations. The transition between these orientations, to a well-ordered A·M·ADP or rigor state, might well generate the strain between the filaments.

AlF$_3$ as an Analog of an Intermediate State of the Cycle. As with any study which attempts to trap an intermediate of the biochemical cycle, it is necessary to assign the trapped

intermediate to the state of the original pathway. For acto–S1 complexes in solution, AlF$_3$·ADP or BeF$_3$·ADP are thought to be analogs of the AM**·ADP·P$_i$ state. There is a 16% increase in fluorescence of an intrinsic tryptophan, which is the same as for the AM**·ADP·P$_i$ state (Maruta et al., 1993; Phan et al., 1993). Second, there is a strong reciprocal coupling between the binding affinities of actin and the ADP·BeF$_3$ nucleotide to S1. In the presence of actin, fluoroberyllate·ADP binding to S1 is reduced by a factor of 100, while in the presence of ADP·BeF$_3$ the affinity of S1 binding to actin is reduced at least 1000-fold to 0.1 mM (Phan et al., 1993). A similar reciprocity of binding was observed for complexes with AlF$_3$ (Maruta et al., 1993), parallelling the behavior of the ADP·P$_i$ complex (Greene & Eisenberg, 1982; Smith & Eisenberg, 1990). Third, the formation of the ternary complexes of A·S1·ADP·AlF$_3$ displays a strong dependence on ionic strength (Maruta et al., 1993); a similar dependence was observed for the A·S1·ADP·P$_i$ complex (Chalovich & Eisenberg, 1986). Finally, AlF$_3$ does not bind to myosin if the γ-phosphate site in the nucleotide binding pocket is occupied (Maruta et al., 1993). Like vanadate, beryllium or aluminum fluoride bind in the same position as the γ-phosphate of hydrolyzed ATP and so mimic the P$_i$ states. There are, however, differences between these P$_i$ analogs; vanadate is thought to stabilize the transition state due to its pentagonal bipyramidal structure; beryllate, on the other hand, has a tetrahedral geometry which is also the most likely structure for AlF$_3$ (Maruta et al., 1993). There must be more subtle differences, since the rate of ternary complex decomposition is faster for BeF$_3$ than for V$_i$, and slowest for AlF$_3$. Nevertheless, there is sound agreement that the ternary complex of A·S1·ADP·AlF$_3$ is a good analog of the AM**·ADP·P$_i$ state.

In muscle fibers, the identification of the trapped state is not as clear. In the absence of Ca^{2+}, there is no attachment, as measured by mechanical stiffness. This is not too surprising since all of the solution studies were performed with unregulated actin, and a more meaningful comparison is that in the presence of Ca^{2+}. The 42% of rigor stiffness observed here, and by Chase et al. (1993), is indicative of the attachment of at least 21% of the myosin heads. [This lower bound for the attached fraction assumes that all of the crossbridges are single-headed, such as those formed in the presence of AMPPNP (Fajer et al., 1988), in which case 21% of the bound myosin heads could account for 42% stiffness.] The EPR lineshape obtained excludes the possibility that these attached heads are A·M·ADP or A·M complexes, which could arise from incomplete saturation with fluoroaluminate nucleotide, due to the decreased affinity in the presence of actin (Phan et al., 1993) or Ca^{2+} (Kraft et al., 1992). Conventional EPR spectra are capable of resolving 1–3% of rigor or ADP heads in the presence of large disorder, due to the characteristic narrow lineshape observed for these heads [see Figure 2 or Fajer (1994)]. No evidence for such a lineshape was found either for the intrinsic heads in fibers (Figure 2) or for the extrinsic heads in decorated fibers (Figure 4); thus, the heads contributing to stiffness are ternary complexes of actin, myosin, and the nucleotide fluoroaluminate. The trapped state(s) is (are) a mixture of detached and attached heads, in agreement with the low affinity of the myosin–nucleotide complex for actin (Phan et al., 1993). The attached heads are not in a rapid equilibrium with the detached heads, since there is little if any dependence of stiffness on the rate of stretch (Chase et al., 1994). Thus, the trapped state is different than the "weakly" attached states observed in low ionic strength relaxing conditions (Brenner et al., 1982; Schoenberg, 1985). Fur-

thermore, this state is Ca^{2+}-regulated, whereas the "weak" binding states are not (Chalovich & Eisenberg, 1986). Clearly, the attached heads correspond to the later states in the cycle, most probably the early "strongly" attached states prior to the tension-generating steps(s), but whether the AlF-induced state is the phosphate state analog is, however, unclear. A recent preliminary report on the orientational distribution in actively contracting fibers found that an increased P_i concentration did not cause increasing head disorder, suggesting that the AlF-induced state might be different from the state induced by phosphate (Zhao & Cooke, 1994b).

Disorder of the Attached Heads. It is rather surprising that the orientational distribution of the myosin heads in these "strongly" attached pre-power stroke states is identical to that of detached myosin heads, or to the heads in the early stages of attachment. Recent attempts to characterize the acto–myosin interface, based on the atomic resolution structure of actin and myosin (Rayment *et al.*, 1993), suggest that the initial attachment is not stereospecific, and involves an electrostatic attraction between the positively charged residues in the upper 50K domain and the negatively charged clusters in the N-terminus of actin. Such an electrostatic attraction does not confine significantly the geometric arrangement of the two proteins in the complex, and a broad distribution of myosin head orientations is observed by EPR (Fajer *et al.*, 1991), by numerous EM studies (Applegate & Flicker, 1987; Frado & Craig, 1992; Walker *et al.*, 1994), and also by X-ray diffraction from fibers (Yu & Brenner, 1989). This disorder is dynamic, with motion on the microsecond time scale as measured by saturation transfer EPR (Fajer *et al.*, 1991). Orientational freedom is greatly restricted upon the formation of strong bonds between actin and myosin, resulting in the stereospecific arrangement of actin and myosin. For example, in the post-power stroke states, the myosin heads display a characteristic arrowhead appearance in electron micrographs. In rigor and ADP, the heads are attached at 40° (Pollard *et al.*, 1993), or at 45° (Walker *et al.*, 1994), with respect to the actin filaments. The tilt disorder, as estimated from EM, is ±9–13°, in agreement with the EPR estimate of ±5° disorder of head tilt and ±7° disorder of head torsion (Fajer, 1994).

The orientation in the intermediate stages is more elusive. The nonhydrolyzable ATP analog AMPPNP has been implied to represent a "strongly" attached pre-power stroke state (Marston *et al.*, 1976), with an orientation different from that in rigor, as observed in the EM of insect flight muscle (Reedy *et al.*, 1983). However, in rabbit psoas muscle, Fajer *et al.* (1988) found that no new orientation of attached heads was induced by AMPPNP but rather a double-headed crossbridge was formed consisting of one head attached as in rigor and the other disordered as in relaxation. Identical findings were reported for psoas fibers in PP_i, another candidate for a pre-power stroke state (Pate & Cooke, 1988). Perhaps most relevant is the time-resolved EM study of head orientation, following the photolysis of caged ATP. Hirose *et al.* (1993) observed a large axial disorder of the heads prior to full tension generation, at 50 ms after the initiation of contraction. It is likely that some of these disordered heads are those observed in this work.

Modeling of Head Mobility. The precise determination of the mobility depends crucially on the estimate of the fraction of attached heads. As there is no spectral resolution in the ST-EPR spectra of the bound and detached heads, one has to rely on an independent measurement of head attachment. The proteolytic digestion method developed by Reisler relies on the protection of the 20/50K junction by attachment to
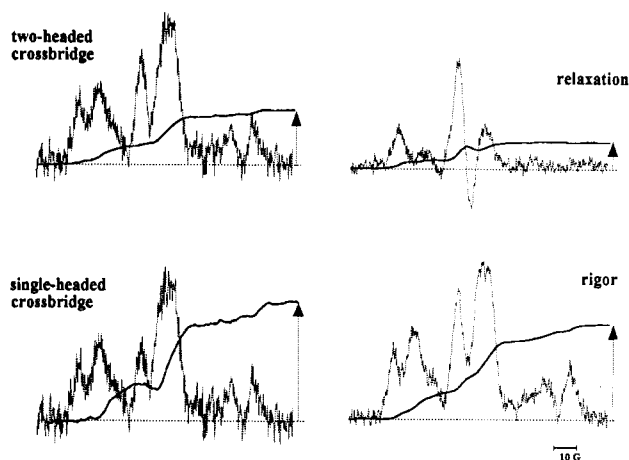

FIGURE 5: Mobility of bound myosin heads. *Left*: ST-EPR difference spectra created by subtraction of a fraction of the relaxed spectrum corresponding to the detached heads: (*top*) the attached fraction is equal to the fraction of the rigor stiffness, two-headed crossbridge; (*bottom*) the attached fraction is half of the stiffness fraction as expected from single-headed crossbridges. *Right*: Relaxed (*top*) and rigor spectra (*bottom*). Superimposed on all spectra is the first integral of ST-EPR; the height of the arrows denotes the relative restriction on mobility in each state.

actin, and the digestion rate is proportional to the fraction of detached heads (Duong & Reisler, 1987). This method was successfully applied to contracting myofibrils (Berger & Thomas, 1993), but presents problems in fiber bundles, in which the digestion might be limited by the diffusion rates of proteolytic enzymes. A less direct method is the measurement of fiber stiffness. The elasticity of muscle fibers was shown to be proportional to the degree of overlap between the thick and thin filaments, establishing proportionality between the number of crossbridges and stiffness (Ford *et al.*, 1981). Thus, if it is assumed that the stiffness is proportional to the number of attached heads (f), and that the heads not contributing to stiffness have the mobility of the relaxed heads, one can estimate the mobility of the putative pre-power stroke heads by subtracting from the ST-EPR (AlF_3/Ca^{2+}) spectrum the $(1 - f)$ fraction of the relaxed spectrum. The difference spectrum (Figure 5) normalized to f has the lineshape and intensity characteristic of a slowly moving species, $\tau_r = 150–400$ μs.

The scenario given above assumes that the measured stiffness originates from the compliance of each bound head and, furthermore, it does not depend on its chemical state. However, the first assumption does not always hold, as in the presence of AMPPNP or PP_i the crossbridges in which only one head of the two-headed myosin molecule was bound to the thin filament were found to be as stiff as the rigor crossbridges in which both heads are attached (Fajer *et al.*, 1988; Pate & Cooke, 1988). If this was the case with AlF_3/Ca^{2+} heads, the bound fraction would be $1/2f$, and the mobility of this population can be estimated from the difference spectrum, $(2V_{AlF/Ca} - fV_{relax})/f$. The integrated intensity of such a difference spectrum (Figure 5) is higher than that for rigor; thus, the attached heads in the single-headed crossbridge would have to be less mobile than the rigor heads, not a likely possibility. Finally, the compliance of the head can well be a function of the chemical state. Yu and co-workers measured changes in the lattice spacing in response to radial forces for a variety of chemical states, and concluded that at least radial stiffness depends critically on the state of the bound nucleotide (Xu *et al.*, 1993). Axial compliance does not necessarily obey

the same trends. Kawai and Zhao (1993) observed nearly constant (within 25%) stiffness of all "strongly" attached heads. Nevertheless, even if we assume that all the heads are attached to thin filaments, and the compliance of each head is 42% of the rigor head, the mobility of these attached heads is considerably slower than the mobility of the detached heads. The restriction on the mobility of the heads is expected from a "strong" binding state. Rigor heads are rigid on the microsecond time scale as measured by ST-EPR (Thomas & Cooke, 1980) or phosphorescence anisotropy decays (Stein *et al.*, 1990). By contrast, "weakly" attached heads displayed a large orientational distribution, accompanied by fast microsecond motion only 20–30% slower than that of detached heads (Fajer *et al.*, 1991). The state observed here corresponds to one of the intermediates between the initial, weak attachment and the final strong rigor bond. Whether or not this intermediate is long- or short-lived during isometric contraction is debatable. A number of transient experiments have revealed that the development of fiber stiffness precedes the development of tension, leading to the proposal of a low-force, "strongly" attached state (Ford *et al.*, 1981; Cecchi *et al.*, 1982), but the kinetic studies of Kawai and Zhao (1993) did not find evidence for such a state during steady-state isometric contraction. According to Kawai's model, the $AM \cdot ADP \cdot P_i$ state (the state populated by the inclusion of free P_i in contracting solutions) is the first force-producing state, with the head generating more force in that state than in subsequent steps. This proposal is seemingly at odds with transient experiments using caged ATP (Hibberd *et al.*, 1985) or the steady-state experiments of Pate and Cooke (1985), in which the addition of phosphate led to decreased tension. It seems that these different techniques are sensing different isomers of $AM \cdot ADP \cdot P_i$: a low- and a high-force state(s). If the isomerization rate and the rate of attachment were comparable, Kawai's oscillatory perturbations might not be able to resolve these two states. However, even if the latter work could not resolve the two states, it does provide an upper bound for the $AM \cdot ADP \cdot P_i$ state(s) of 20% of the total crossbridge population. This low value might explain why so few of these immobile crossbridges are observed during steady-state contraction. Using time-resolved phosphorescence anisotropy decays, Thomas and collaborators observed a population of bound heads with restricted mobility ($\tau_r \approx 25$–600 μs) in isometric contraction (Stein *et al.*, 1990), but their more recent ST-EPR measurements on cross-linked myofibrils seem to indicate that the bound heads are much more mobile, $\tau_r = 3$ μs (Berger & Thomas, 1993). The fraction of immobile heads may well be too small, or the $AM \cdot ADP \cdot P_i$ state too short-lived, to affect the weighted average observed during steady-state contraction.

In conclusion, we believe we have shown that the myosin heads prior to the force-generating step are disordered and significantly less mobile than detached or "weakly" bound heads. Ordering of the heads may well be the structural event driving the generation of force.

ACKNOWLEDGMENT

REFERENCES

Applegate, D., & Flicker, P. (1987) *J. Biol. Chem. 262*, 6856–6863.

Barnett, V. A., & Thomas, D. D. (1984) *J. Mol. Biol. 179*, 83–102.

Barnett, V. A., & Thomas, D. D. (1989) *Biophys. J. 56*, 517–523.

Berger, C. L., & Thomas, D. D. (1993) *Biochemistry 32*, 3812–3821.

Brenner, B., Schoenberg, M., Chalovich, J. M., Greene, L. E., & Eisenberg, E. (1982) *Proc. Natl. Acad. Sci. U.S.A. 79*, 7288–7291.

Cecchi, G., Griffith, P. J., & Taylor, S. (1982) *Science 217*, 70–72.

Chalovich, J. M., & Eisenberg, E. (1986) *J. Biol. Chem. 261*, 5088–5093.

Chase, P. B., Martyn, D. A., Kuschmerick, M. J. & Gordon, A. M. (1993) *J. Physiol. 460*, 231–246.

Chase, P. B., Martyn, D. A., & Hannon, J. D. (1994) *J. Muscle Res. Cell Motil. 15*, 119–129.

Duong, A. M., & Reisler, E. (1987) *J. Biol. Chem. 262*, 4124–4128.

Fajer, P. G. (1994) *Proc. Natl. Acad. Sci. U.S.A. 91*, 937–941.

Fajer, P., & Marsh, D. (1982) *J. Magn. Reson. 49*, 212–224.

Fajer, P. G., Fajer, E. A., Brunsvold, N. J., & Thomas, D. D. (1988) *Biophys. J. 53*, 513–524.

Fajer, P. G., Fajer, E. A., Matta, J. J., & Thomas, D. D. (1990a) *Biochemistry 29*, 5865–5871.

Fajer, P. G., Fajer, E. A., & Thomas, D. D. (1990b) *Proc. Natl. Acad. Sci. U.S.A. 87*, 5538–5542.

Fajer, P. G., Fajer, E. A., Schoenberg, M., & Thomas, D. D. (1991) *Biophys. J. 60*, 642–649.

Ford, L. E., Huxley, A. F., & Simmons, R. M. (1981) *J. Physiol. (London) 311*, 219–249.

Frado, L. L., & Craig, R. (1992) *J. Mol. Biol. 223*, 391–397.

Greene, L. E., & Eisenberg, E. (1982) *Methods Enzymol. 85*, 709–724.

Hibberd, M. G., Dantzig, J. A., Trentham, D. R., & Goldman, Y. E. (1985) *Science 228*, 1317–1319.

Hirose, K., Lenart, T. D., Murray, J. M., Franzini-Armstrong, C., & Goldman, Y. E. (1993) *Biophys. J. 65*, 397–408.

Huxley, H. E. (1969) *Science 164*, 1356–1365.

Kraft, T., Yu, L. C., Kuhn, H. J., & Brenner, B. (1992) *Proc. Natl. Acad. Sci. U.S.A. 89*, 11362–11366.

Marston, S. B., Rodger, C. D., & Tregear, R. T. (1976) *J. Mol. Biol. 104*, 263–276.

Maruta, S., Henry, G. D., Sykes, B. D., & Ikebe, M. (1993) *J. Biol. Chem. 268*, 7093–7100.

Offer, G., & Elliott, A. (1978) *Nature 271*, 325–329.

Pate, E., & Cooke, R. (1985) *Biophys. J. 47*, 773–780.

Pate, E., & Cooke, R. (1988) *Biophys. J. 53*, 561–573.

Pate, E., Riley, J., & Cooke, R. (1992) *Biophys. J. 61*, 268a.

Phan, B., & Reisler, E. (1992) *Biochemistry 31*, 4787–4793.

Phan, B. C., Faller, L. D., & Reisler, E. (1993) *Biochemistry 32*, 7712–7719.

Pollard, T. D., Bhandari, D., Maupin, P., Wachsstock, D., Weeds, A. G., & Zot, H. G. (1993) *Biophys. J. 64*, 454–471.

Rayment, I., Holden, H. M., Whittaker, M., Yohn, C. B., Lorenz, M., Holmes, K. C., & Milligan, R. A. (1993) *Science 261*, 58–65.

Reedy, M. K., Goody, R. S., Hofmann, W., & Rosenbaum, G. (1983) *J. Muscle Res. Cell Motil. 4*, 25–53.

Schoenberg, M. (1985) *Biophys. J. 48*, 467–475.

Schoenberg, M. (1993) *Adv. Biophys. 29*, 55–73.

Schrumpf, M., & Wray, J. (1992) *J. Muscle Res. Cell Motil. 13*, 254.

Smith, S. J., & Eisenberg, E. (1990) *Eur. J. Biochem. 193*, 69–73.

Squier, T., & Thomas, D. D. (1986) *Biophys. J. 49*, 921–935.

Stein, R. A., Ludescher, R. D., Dahlberg, P. S., Fajer, P. G., Bennett, R. L., & Thomas, D. D. (1990) *Biochemistry 29*, 10023–10031.

Thomas, D. D., & Cooke, R. (1980) *Biophys. J. 32*, 891–906.

Thomas, D. D., Dalton, L. R., & Hyde, J. S. (1976) *J. Chem. Phys. 65*, 3006–3024.

Thomas, D. D., Ishiwata, S., Seidel, J. C., & Gergely, J. (1980) *Biophys. J. 32*, 873–889.

Tregear, R. T., Wakabayashi, K., Tanaka, H., Iwamoto, H., Reedy, M. C., Reedy, M. K., Sugi, H., & Amemiya, Y. (1990) *J. Mol. Biol. 214*, 129–141.

Walker, M., White, H., Belknap, B., & Trinick, J. (1994) *Biophys. J. 66*, 1563–1572.

Weeds, A. G., & Taylor, R. S. (1975) *Nature (London) 257*, 54–56.

Werber, M. M., Peyser, Y. M., & Muhlrad, A. (1992) *Biochemistry 31*, 7190–7197.

Xu, S., Brenner, B., & Yu, L. C. (1993) *J. Physiol. 461*, 283–299.

Yu, L. C., & Brenner, B. (1989) *Biophys. J. 55*, 441–453.

Zhao, L., Naber, N., & Cooke, R. (1994a) *Biophys. J.* (submitted for publication).

Zhao, L., Naber, N., & Cooke, R. (1994b) *Biophys. J. 66*, 192a.